Elastic scattering of ^{16}O by even mass nickel isotopes*

Leon West, Jr., K. W. Kemper, and N. R. Fletcher
Department of Physics, The Florida State University, Tallahassee, Florida 32306
(Received 29 August 1974)

The angular distributions of ^{16}O elastically scattered from enriched targets of even-mass nickel isotopes have been measured for $E_{^{16}O} = 36$ to 56 MeV. A four parameter optical model is used to describe the data and the parameter ambiguities are discussed in detail. A potential folding calculation provides an equally good representation of the data and yields a set of equivalent optical model parameters which are within the parameter ambiguity relationships discussed. The ^{16}O + nucleon real potential necessary to describe the data through the folding procedure is less than one-half the value derived from ^{16}O + nucleon scattering measurements.

[NUCLEAR REACTIONS $^{58,60,62,64}Ni(^{16}O,^{16}O)$, measured $\sigma(\theta, E)$, $E = 36$ to 56 MeV. Four parameter optical model and folded optical model descriptions.]

I. INTRODUCTION

Although the first heavy ion reaction experiments were performed well over a decade ago, the simplest of these, elastic scattering, is still of principal importance not only as an intermediate step towards the understanding of more complicated interactions between complex nuclei, such as those involving nucleon transfer, but also because it provides an opportunity to investigate the applicability of both macroscopic and microscopic interaction models for a relatively simple reaction. The present work is an investigation of the energy dependence and the parameter ambiguities encountered in application of the four parameter optical model to the elastic scattering of ^{16}O from the even mass number stable nickel isotopes. The formulation and calculation of a single folding description of the $^{16}O+^{58}Ni$ scattering is also presented in which the optical model description of ^{16}O+ nucleon scattering is used in an integration over the target mass density.

Compared to the amount of experimental and calculational information available for the interaction of light ions ($A \leq 4$) with intermediate mass nuclides, there is still relatively little information available on the interaction between heavy ions and nuclei with mass greater than ~30. One of the first reports of heavy ion scattering, by McIntyre, Baker, and Watts,[1] included the scattering of ^{16}O from a natural nickel target at 158 MeV but no quantitative analysis was performed.

In much of the more recently reported elastic scattering data a four parameter optical model has been found to satisfactorily describe angular distributions and yield curves. There is, however, a considerable question about the reliability of the ratio of imaginary well depth to real well depth (W/U) as derived from these analyses. In the work of Orloff and Daehnick,[2] on the elastic scattering of ^{16}O by ^{48}Ti, ^{40}Ca, and ^{27}Al at bombarding energies of 40 to 48 MeV, the deduced values of real potential well depth, U, differed somewhat with each incident energy, but the extracted values for the imaginary well depth, W, exhibited quite an erratic energy dependence. The ratio W/U was found to vary between 5 and 50% in a nonsystematic way. Other results combined[3-5] have also shown the values of W/U to range from less than 10% to greater than 50%.

In an effort to establish the energy dependence of the real and imaginary well depths, angular distributions for the elastic scattering of ^{16}O by $^{58,60,62,64}Ni$ were measured at bombarding energies from 36 MeV to as high as 56 MeV in 2 MeV steps. The energy dependence of the well depths and the question as to whether large or small absorption is more appropriate are considered in Sec. III A. Some possible causes for the deduced variability of the ratio W/U are also discussed in this section. In Sec. III B the ambiguities in the optical model parameters are examined and the apparent constancy of extracted values for the Coulomb barrier height and radius are shown to be but a moderate extension of the standard Igo ambiguities.[6]

Although the conventional optical model has provided adequate parameterization of cross sections of the elastic scattering of ^{16}O from various nuclei, this is in a sense fortuitous. In the optical model the scattering of two nuclei is considered to be a model equivalent to the scattering of a point nucleus from a potential well. The application of the model historically progressed from describing neutron cross sections to describing the scattering of protons, α particles, and other light nuclei. Now it has even been applied to parametrize the elastic scattering of a projectile as massive as an oxygen nucleus. In light of recent advances in the

use of folded potentials to describe α-particle scattering,[7] the ^{16}O scattering question should also be considered from a more microscopic point of view.

In the folded potential approach, the interaction between two complex nuclei is assumed to be determined by a sum of two-body nucleon-nucleon potentials, or a sum of effective nucleon-projectile potentials. The summation over nucleons is approximated as an integration over the matter distribution of the pertinent nucleus. The algebra of folded potentials is considered in Sec. III C, the various parameters arising in the folded potential description are explained, and the results of an application to the $^{16}O+^{58}Ni$ scattering are discussed.

II. EXPERIMENTAL PROCEDURE

A negatively charged O^- or OH^- beam from a Heinicke radial extraction ion source[8] was injected at 80 keV into the Florida State University model S-FN tandem Van de Graaff accelerator for production of oxygen beams in the energy range 36 to 56 MeV. The beam impinged upon isotopically enriched nickel metal targets of 30 to 80 μg/cm^2 thickness which were vacuum deposited into thin carbon backings.

An array of 8 to 16 Si surface barrier detectors of 100 μm depletion depth mounted at 10° intervals in a precision scattering chamber was used to measure the elastic and inelastic scattering angular distributions. No particle identification techniques were necessary. In order to prolong detector usefulness, those forward angle detectors which experienced localized radiation damage in a relatively short period of time due to a high count rate, were mounted off center with respect to the small circular collimators. These detectors were then rotated periodically to expose an undamaged portion of the silicon crystal.

Typical energy spectra are displayed in Fig. 1. Energy resolution ranged from 250 to 500 keV. In many cases, it was found necessary to use a Gaussian line shape peak fitting routine to extract the inelastic yield when it was small and superimposed upon the approximately exponential low-energy tail of the much larger elastic yield. The

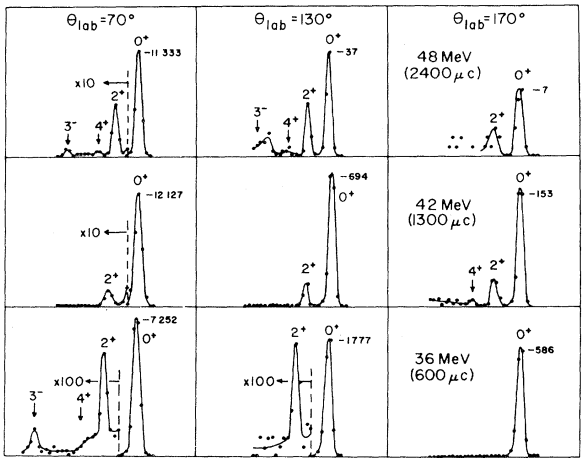

FIG. 1. Comparative spectra for $^{16}O+^{58}Ni$ at several laboratory energies and angles with the amount of collected charge indicated at each energy. Peaks corresponding to states of ^{58}Ni are labeled by spin and parity. The number of counts in the peak channel is shown.

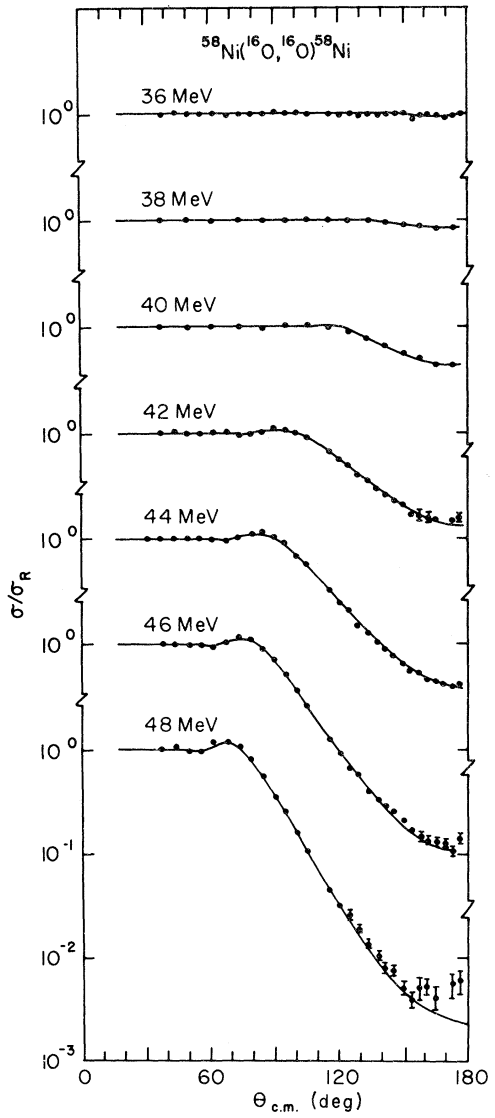

FIG. 2. Measured elastic scattering cross sections for $^{58}Ni(^{16}O, ^{16}O)^{58}Ni$ at several bombarding energies. The solid lines are calculated cross sections for the geometry parameter values of $r_0 = 1.22$ fm and $a = 0.50$ fm, as explained in the text. The real and imaginary well depths at each energy are illustrated in Fig. 6.

error bars shown in the angular distributions, Figs. 2 through 5, represent cumulative relative errors from background subtraction, line shape fitting, and statistical effects. A report of the inelastic cross sections and an accompanying analysis is the subject of a subsequent publication.[9]

III. ANALYSIS OF ELASTIC SCATTERING

A. Optical model analysis with fixed geometric parameters

The elastic scattering angular distributions measured at several bombarding energies between 36 and 56 MeV are shown in Figs. 2 through 5. The solid curves in these figures are the results of a four parameter optical model calculation using a modified version of the computer program JIB.[10] The potential used in the calculation has the form:

$$V_{OM}(r) = -(U + iW)(1 + e^{x})^{-1} + V_c(r), \quad (1)$$

where

$$x = (r - R)/a$$

and

$$V_c(r) = Z_P Z_T e^2 \begin{cases} \frac{1}{2R_C}\left(3 - \frac{r^2}{R_C^2}\right), & \text{for } r \leq R_C \\ \frac{1}{r}, & \text{for } r > R_C . \end{cases} \quad (2)$$

The nuclear radius is written in terms of the radius parameter, r_0, as $R = r_0(A_T^{1/3} + A_P^{1/3})$. The calculated results are insensitive to the Coulomb radius and therefore throughout we have set $R_C \equiv R$.

In the initial parametrization the real and imaginary well depths, U and W, were allowed to vary while the radius and diffuseness parameters, r_0 and a, were held fixed until the value of χ^2, defined as

$$\chi^2 = \sum_{i=1}^{n} \left(\frac{\sigma_{exp} - \sigma_{calc}}{\Delta\sigma_{exp}} \right)_i^2 ,$$

had a minimum value. The fixed radius parame-

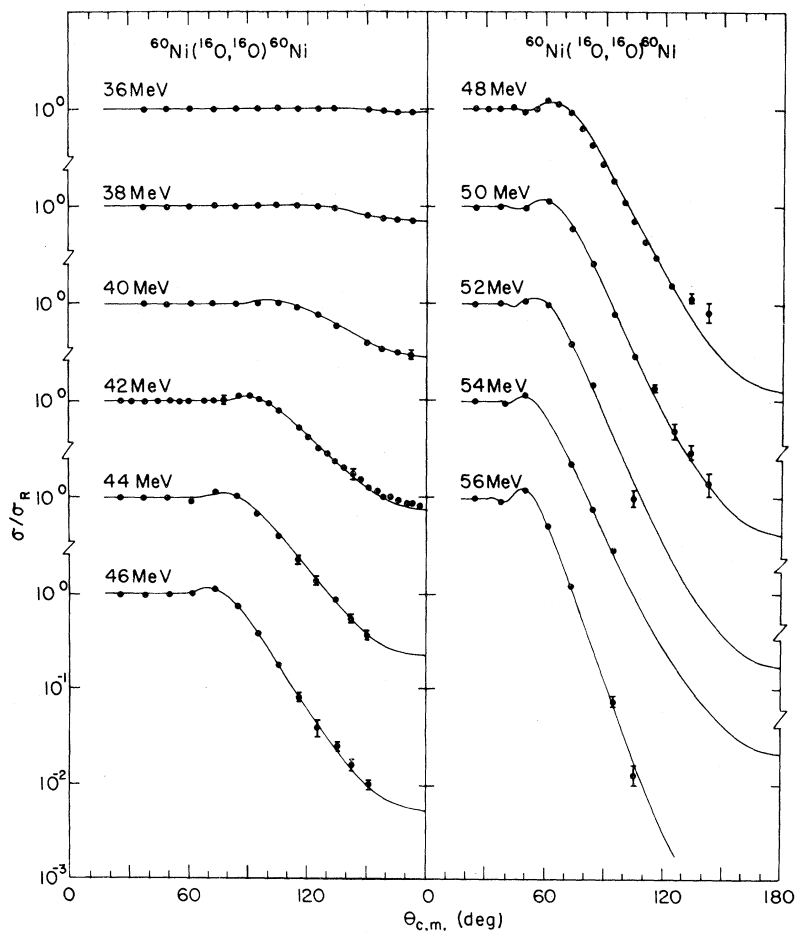

FIG. 3. Measured elastic scattering cross sections for $^{60}Ni(^{16}O, ^{16}O)^{60}Ni$ at several bombarding energies. (See caption, Fig. 2.)

ter was chosen as $r_0 = 1.22$ fm. A fixed diffuseness value of $a = 0.5$ fm appears to result in the best reproduction of the experimental cross sections when the data from all targets, $A_T = 58$ to 64, are considered. A smaller value of $a = 0.4$ fm for ^{58}Ni did result in a reduction in the value of χ^2 of about 10%; however, such a value is entirely too small for the other target nuclei. Typical values of χ^2 divided by the number of degrees of freedom were 2 to 5.

The energy dependence of the extracted real and imaginary potentials is shown in Fig. 6. The uncertainties, ΔU shown by the error bars in Fig. 6, assigned to the potential U are determined from the criterion,[11] $\chi^2(U + \Delta U, W) = \chi^2_{\min}(U, W) + 1$. A similar criterion is used to determine the uncertainty in W. The large value of the ratio, $W/U \sim 30\%$, indicates that the ^{16}O+Ni scattering system is highly absorptive at these energies. A similar result was obtained by Obst, McShan, and Davis[5] for the elastic scattering of ^{16}O by ^{56}Fe, ^{70,74}Ge, and ^{90}Zr for similar bombarding energies.

Although the values shown in Fig. 6 were obtained for $r_0 = 1.22$ fm and $a = 0.50$ fm very comparable descriptions of the data can be obtained at $E_{\text{lab}} = 48$ MeV by fixing $r_0 = 1.22$ fm U and W at 93 and 34 MeV, respectively, and allowing the diffuseness to assume the values 0.500, 0.513, 0.519, and 0.532 fm for the different mass targets, $A_T = 58$, 60, 62, and 64, respectively. It is found that these diffuseness values also tend to eliminate the energy dependence in U.

There are two aspects of the quantity and quality of the elastic scattering data which critically affect the ratio W/U. The results cited from the following examples are thought to have general applicability for the ^{16}O+Ni scattering systems; however, no complete survey of the effects was carried out. Both of the effects were noted with geometric parameters of $a = 0.50$ fm and $r_0 = 1.25$

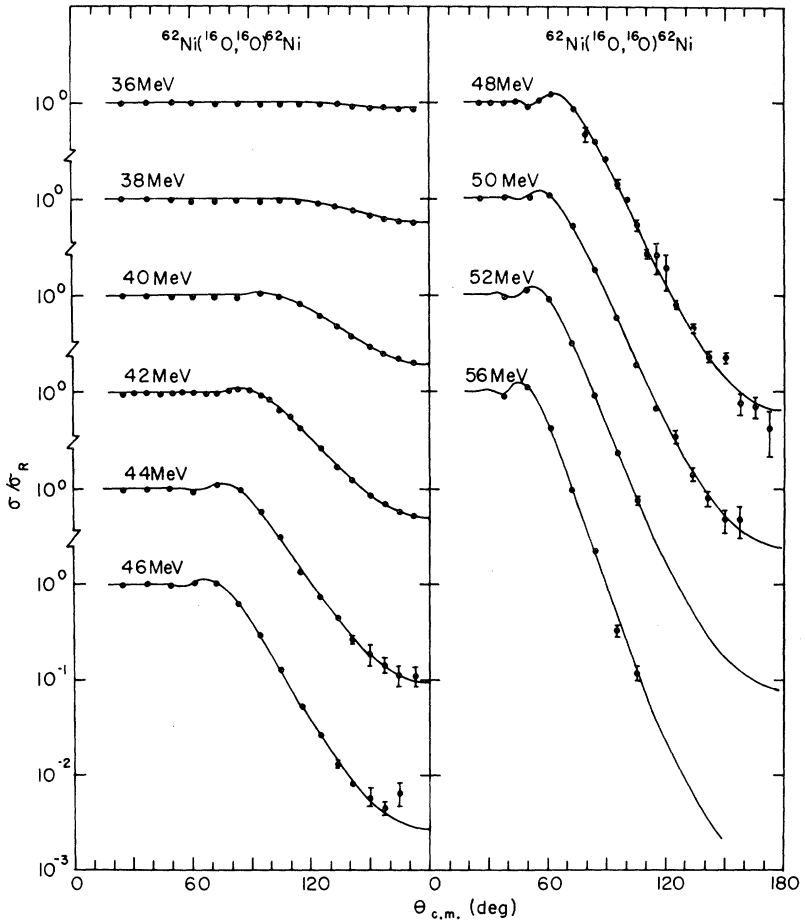

FIG. 4. Measured elastic scattering cross sections for ^{62}Ni(^{16}O, ^{16}O)^{62}Ni at several bombarding energies. (See caption, Fig. 2.)

fm, rather than 1.22 fm used above.

The first involves the absolute cross section measurement. For $^{16}O+^{58}Ni$ at $E_{lab}=42$ MeV a set of potentials of minimum χ^2 is $U=60$ MeV, $W=15$ MeV. A 3% difference in the absolute scattering cross section would have yielded the values, $U=61$ MeV, $W=20$ MeV, making W/U critically dependent upon normalization.

The second effect concerns the quantity and quality of scattering data at back angles. For the $^{16}O+^{58}Ni$ scattering at 48 MeV, potential values of $U=60$ MeV, $W=25$ MeV are obtained when all of the 48 MeV angular distribution data of Fig. 2 are used in the χ^2 minimization. If, however, the data are truncated at 120° the resulting potentials are $U=60$ MeV, $W=10$ MeV. In this latter case where a reproduction of the low yield back angle scattering is not required the fit is actually better in the region of 50° to 80°, near the grazing angle. It is this region where an optical model description is most critical if the parameters are to be used in a distorted-wave Born-approximation (DWBA) calculation for a transfer reaction and this may be a partial explanation of why descriptions of scattering data display a preference for high absorptions, whereas the DWBA descriptions of transfer data display a preference for small values of W.

B. Ambiguities in the optical model parameters

With the geometric parameters fixed, as discussed in the previous section, there are no minima in the map of $\chi^2(U,W)$ other than the ones reported, that is, there are no discrete ambiguities. A variety of continuous ambiguities are noted, however, when a true four parameter (U,W,r_0,a) optical model is used. These ambiguities are contained in the distant approximation to the Woods-Saxon potential $r \gg R$. The real part of the optical

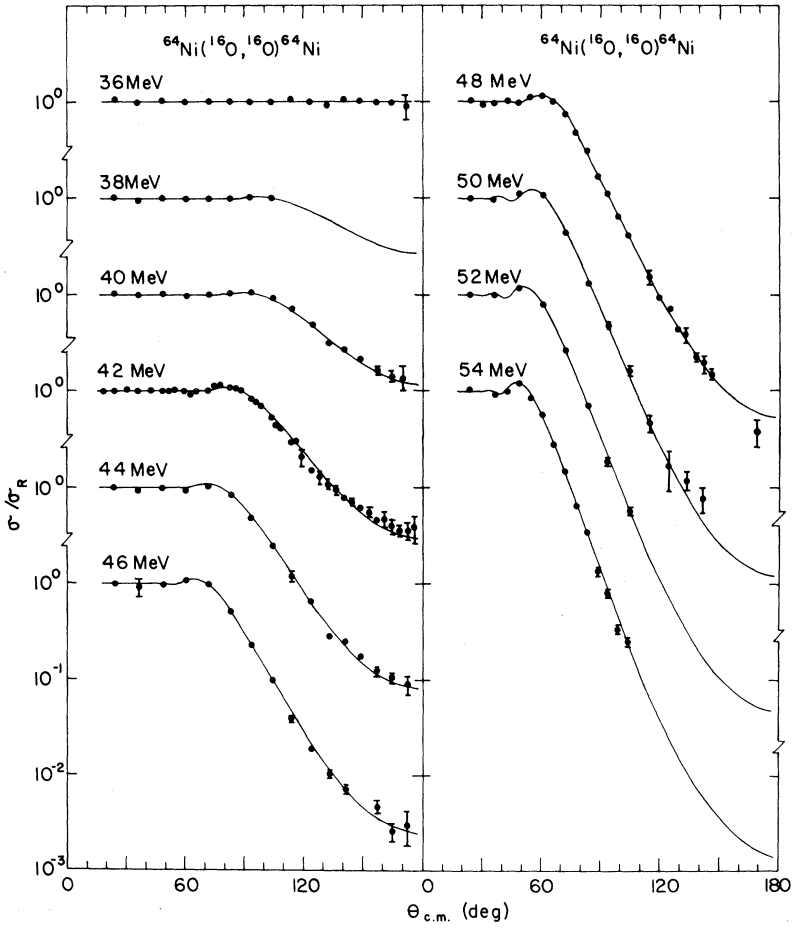

FIG. 5. Measured elastic scattering cross sections for ^{64}Ni(^{16}O, ^{16}O)^{64}Ni at several bombarding energies. (See caption, Fig. 2.)

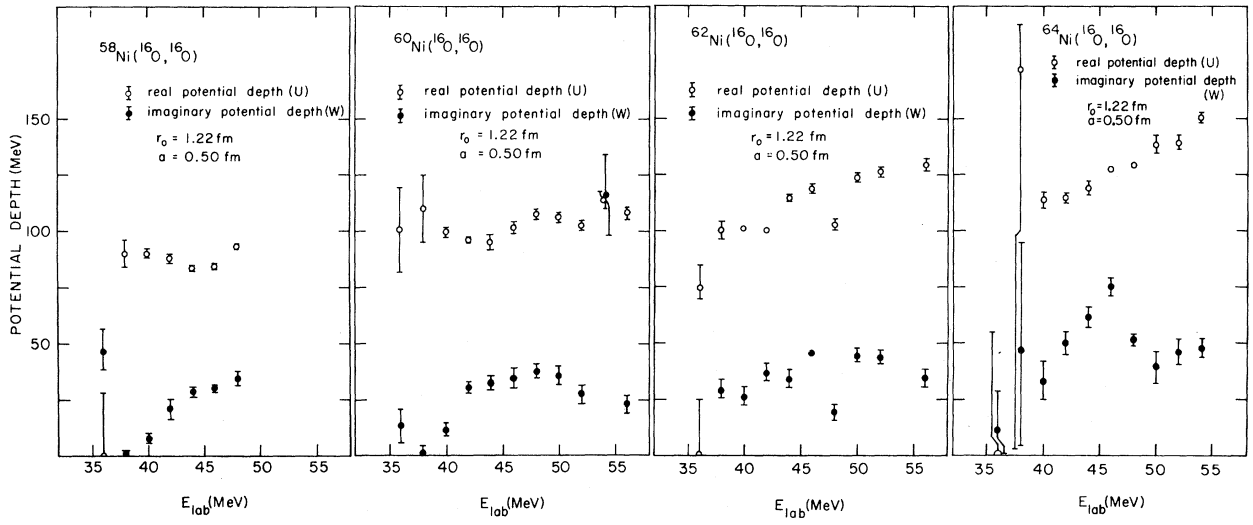

FIG. 6. The values of real and imaginary potential well depths, U and W, respectively, as functions of laboratory energy for the elastic scattering of ^{16}O from ^{60}Ni, ^{62}Ni, and ^{64}Ni.

model potential becomes,

$$\mathrm{Re}\{V_{\mathrm{OM}}(r)\} \cong -Ue^{(R/a)}e^{-(r/a)} + V_c(r)\,.$$

It is apparent that for a fixed value of the diffuseness a, any combination of U and R which satisfies the relationship $U\exp(R/a) = C_u$, a constant, will produce an equivalent real part of the optical potential when the distant part of the optical model potential is primary in producing the scattering effects. This U, r_0, a ambiguity was first elucidated by Igo[6] for α-particle scattering. The Igo ambiguity is clearly evident in the results of optical model calculations for the $^{16}O+^{58}Ni$ scattering at 48 MeV with $a = 0.50$ fm as shown in Fig. 7. Not only does the Igo ambiguity describe the behavior of U vs r_0 over three orders of magnitude in U, but also the variations in W are well described for $r_0 \leq 1.25$ fm, resulting in the ratio W/U having a constant value. For the generation of optical model descriptions of the $^{16}O+Ni$ elastic scattering data, the values found for the Igo constants, C_u and C_w, evaluated for $a = 0.50$ fm, are listed in Table I.

As a slight extension of the three parameter Igo ambiguity in U, r_0, and a, it has been noted[4,5] that the sensitive region of the potential can be described by two nearly unique quantities; the barrier height V_B, the maximum of the total real optical potential, and the barrier radius, R_B, the radius at which this maximum occurs. The uniqueness of V_B is illustrated throughout the Igo ambiguity for $a = 0.50$ fm in Fig. 7. The values of barrier height and radius extracted for the four Ni isotopes are

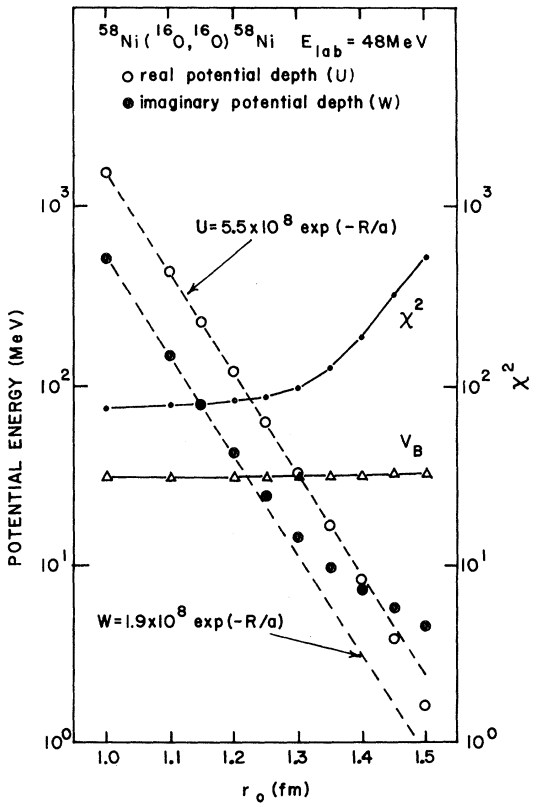

FIG. 7. The values of the real and imaginary potential well depths for which χ^2 is a minimum for different values of r_0. The corresponding value of the Coulomb barrier height V_B is also shown. The diffuseness value is $a = 0.50$ fm. The solid lines are to guide the eye.

TABLE I. For $^{A}Ni(^{16}O, ^{16}O)$, the Igo constants, as defined in the text, which best reproduce the elastic scattering cross section for $^{A}Ni(^{16}O, ^{16}O)^{A}Ni$ at a bombarding energy of 48 MeV. The diffuseness value is $a = 0.50$ fm.

A	C_U (10^8 MeV)	C_W (10^8 MeV)
58	5.47	1.90
60	7.05	2.45
62	7.47	1.30
64	10.45	4.23

shown in Fig. 8. The barrier radius values are described in terms of target and projectile mass numbers in the figure by either of two straight lines. (An earlier illustration of a similar mass dependence of R_B is incorrectly designated in Ref. 4, page 223.)

The connection between the Igo ambiguity and the uniqueness of V_B and R_B is noted by writing,

$$V_B = \mathrm{Re}\{V_{\mathrm{OM}}(R_B)\} = -\frac{U}{1+\exp[(R_B - R)/a]} + V_c(R_B),$$

and since R_B is considerably greater than R, ($R_B \sim R + 4a$), we have the approximate relation,

$$V_B \simeq -U\exp\left(\frac{R - R_B}{a}\right) + V_c(R_B).$$

The foregoing expression not only includes the Igo ambiguity but also indicates that any set of values of real potential U and diffuseness a which satisfies the restriction,

$$U\exp\left(\frac{R - R_B}{a}\right) = C_B,$$

a constant for fixed R, will constitute an equivalent set, provided that knowledge of V_B and R_B is sufficient to determine the real part of the potential. The fulfillment of this requirement has already been demonstrated in Figs. 7 and 8. The resulting continuous ambiguity in parameters U and a is illustrated in Fig. 9 where indeed the value of $\ln(U)$ is a linear function of $(1/a)$ with $C_B = 1.88$, while the barrier height V_B remains constant. For the establishment of the value of C_B, the values of R and R_B are 7.80 and 9.75 fm, respectively.

C. A folded potential calculation

In an attempt to more accurately account for the finite size of the projectile, and to try to avoid the parameter ambiguities of the conventional optical model the use of a folded potential was investigated. In the folded potential approach,[12,13] the potential interaction between a projectile and a target is written in terms of a nucleon-nucleon interaction V_{NN} as

$$V(\vec{r}) = \int_T \int_P \rho_P(\vec{r}_P) V_{NN}(|\vec{r} + \vec{r}_P - \vec{r}_T|)\rho_T(\vec{r}_T) d\vec{r}_P d\vec{r}_T,$$

where $\vec{r}$ is the vector between the two centers of mass, $\vec{r}_T$ is the position vector of a nucleon in the target relative to the center of mass of the target, and $\vec{r}_P$ is defined similarly to $\vec{r}_T$. The two matter

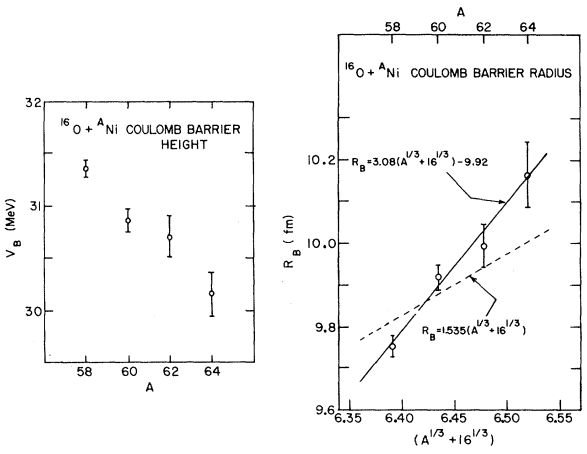

FIG. 8. The Coulomb barrier height V_B and the Coulomb barrier radius R_B as determined from optical model parametrization of $^{58,60,62,64}Ni(^{16}O, ^{16}O)$. The uncertainties in the parameters V_B and R_B are the standard deviations as calculated from the spread about the mean of the individual values for each bombarding energy.

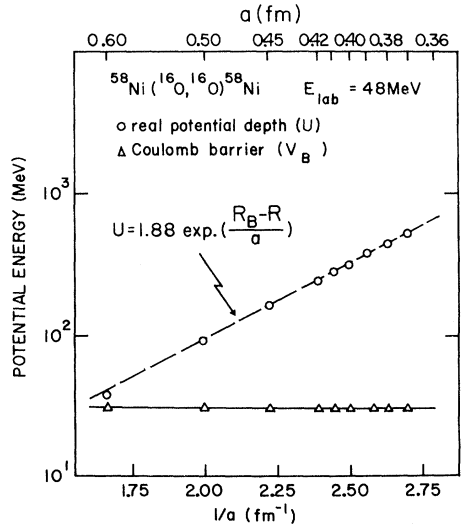

FIG. 9. The real potential well depth which best describes the $^{58}Ni(^{16}O, ^{16}O)^{58}Ni$ angular distribution at a bombarding energy of 48 MeV, as a function of diffuseness with $r_0 = 1.22$ fm. The corresponding values of the Coulomb barrier height are also shown.

distributions for the target and projectile, ρ_T and ρ_P, are assumed to be independent. Since the integrals involve spatial overlap of the two distributions, the Pauli exclusion principle is being neglected. This neglect will overestimate the nucleus-nucleus potential in the interior; however, as shown in the previous sections, the interior region is unimportant for elastic scattering of $^{16}O+Ni$ at these energies.

An approximation to the above equation is obtained by considering the nucleon-projectile optical model potential V_{NP}, folded through the target nucleus. This one step folding procedure is then effected by an integration over target coordinates and the projectile-nucleus potential[7,13,14] and is written as

$$V(\vec{r}) = \int_T V_{NP}(|\vec{r} - \vec{r}_T|)\rho_T(\vec{r}_T)d\vec{r}_T \,. \tag{3}$$

This single fold form is much easier to evaluate numerically and can be used to determine if use of the folding potential is strongly justified.

The two functions in the integrand, V_{NP} and $\rho_T(\vec{r}_T)$, are expanded in a Legendre series[15] in such a manner that the $L=0$ term of $V(\vec{r})$ represents the folding of the familiar Woods-Saxon form for $V_{NP}(r')$ with a Woods-Saxon density distribution. The details of the procedure for application of the $L=2$ part to a folding calculation for the inelastic scattering will be presented at a later date.[9] For the elastic scattering we merely write,

$$V_{NP}(r') = -\frac{U_{NP}}{1+\exp[(r'-R_{NP})/a_{NP}]} \,,$$

where

$$r' = (r^2 + r_T^2 + 2rr_T\cos\theta)^{1/2}$$

and

$$\rho_T(r_T) = \frac{\rho_T^0}{1+\exp[(r_T - R_T)/a_T]} \,.$$

The constant ρ_T^0 is determined by the condition that the number of nucleons in the target contributing to the scattering is given as the target mass number A_T, and therefore

$$\rho_T^0 = \frac{3A_T}{4\pi R_T^3}\left[1+\left(\frac{\pi a_T}{R_T}\right)^2\right]^{-1} \,.$$

Whenever the above folded potential form is used as the real nuclear part of the optical model potential in this work, the imaginary part of the potential is still parametrized in the conventional Woods-Saxon form of Eq. 1. It is felt that since the imaginary potential is strictly a phenomenological potential used to take into consideration open channels not explicitly accounted for in the optical model, the most simple parametrization of the imaginary potential is sufficient. The Coulomb potential term used is still that of the simple uniform charge distribution form of Eq. (2) with $R_c = R$ as before.

In the evaluation of the real part of the projectile + target nucleus potential from Eq. (3), the geometric parameter values for the nucleon + projectile potential are taken as $r_{NP} = 1.25$ fm and a_{NP}

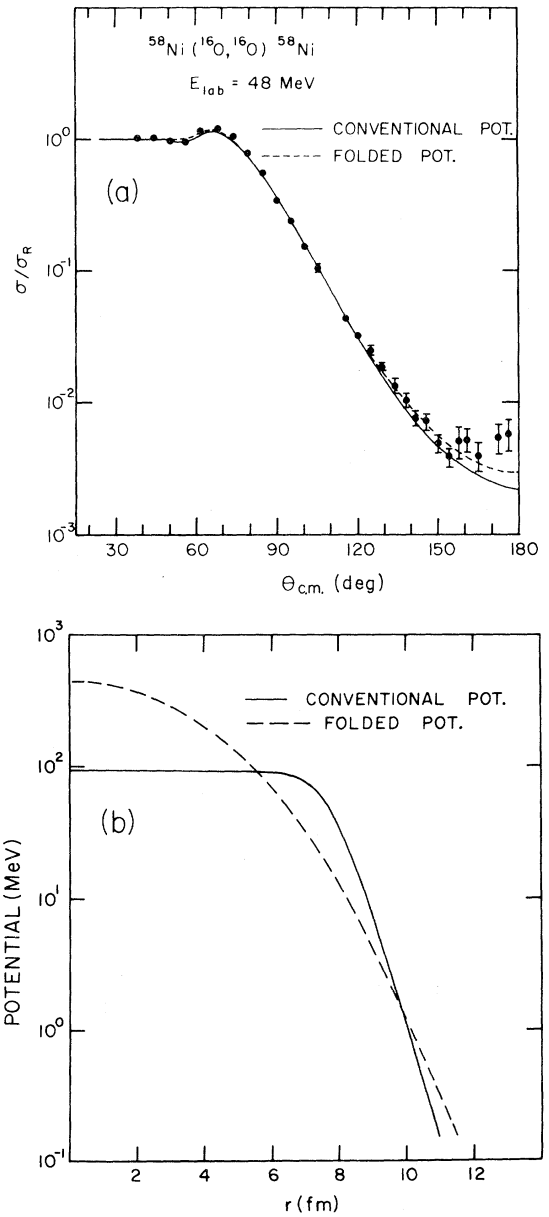

FIG. 10. A folded potential and the resulting calculated cross section compared to a conventional potential and corresponding cross section for ^{58}Ni(^{16}O, ^{16}O)^{58}Ni.

= 0.64 fm in accordance with the values which describe $p + ^{16}$O elastic scattering.[16] The target nucleus matter distribution parameters $r_T = 1.06$ fm and $a = 0.57$ fm, are those determined by electron scattering.[17] The imaginary potential and Coulomb radius in the folded calculation are assigned the same values as used in the conventional calculation to facilitate a comparison. In the folded potential calculation the internucleus effective nucleon + projectile real well depth U_{NP} is allowed to vary until χ^2 is minimized.

A cross section calculation for which the folding procedure has been used is compared to data and to a conventional calculation in Fig. 10(a), for the scattering system ^{16}O + ^{58}Ni at a bombarding energy of 48 MeV. The geometric and potential parameters for the conventional calculation are those given in Sec. III A and Fig. 6. The value of U_{NP} for which χ^2 attained a minimum value in the folded calculation is $U_{NP} = 19.5$ MeV.

As Fig. 10(a) shows, the cross section calculated with the folded potential is virtually identical to the results of the conventional optical model. The rise of the experimental cross section above the Rutherford cross section between 60 and 70° is reproduced slightly better and some improvement occurs in predicting the magnitude and slope of the experimental cross section between 140 and 180°. χ^2 for the folded potential calculation is 15% lower than that for the conventional case. A similar folded potential calculation for ^{16}O + ^{58}Ni at 42 MeV lab energy resulted in χ^2 slightly greater than that for a conventional potential calculation. At this lab energy also, the best value of the nucleon + projectile potential is $U_{NP} = 19.5$ MeV.

A matter for concern might be the fact that the nucleon-projectile well depth of 19.5 MeV results in the best description of the data, while proton + ^{16}O real well depth of approximately 50 MeV best describes proton scattering from ^{16}O.[16] If the value of U_{NP} is fixed at 50 MeV with $r_{NP} = 1.25$ fm and $a_{NP} = 0.64$ fm, the cross section looks similar to those of Fig. 10(a) but is shifted about 10° toward smaller angles. The rise above the Rutherford cross section in this case occurs near 55°. Changing the imaginary potential parameter values has little or no effect upon the location of the rise above the Rutherford cross section. A reasonable fit to the data can be obtained when $U_{NP} = 50$ MeV, $r_{NP} = 1.1$ fm, and $a_{NP} = 0.50$ fm. This value of r_{NP} is another value frequently used to describe nucleon + ^{16}O scattering, but the diffuseness value is smaller than usual values.[16]

The folded and conventional potentials which lead to the cross sections are compared in Fig. 10(b). The two potentials, which have been used to produce nearly equivalent cross sections, have the same value at the radius $r = 9.90$ fm. This feature is a part of the continuous three parameter Igo ambiguity in U, r_0, and a, as discussed in Sec. III B and has also been noted for ^{3}He and α-particle scattering.[18] The folded potential of Fig. 10(b) can be simulated by a Woods-Saxon potential with the same slope and magnitude near the radius of 9.90 fm by the use of the parameter values: $U = 22$ MeV, $r_0 = 1.22$ fm, and $a = 0.78$ fm. These values yield an Igo constant of $C_B = 1.81$, which is in good agreement with the value given in Fig. 9, further demonstrating that the effect of this folded potential can be described within the extended Igo ambiguity.

IV. CONCLUSIONS

As has been observed by other authors,[3-5] the four parameter optical model provides an adequate phenomenological description of the ^{16}O + Ni elastic scattering data in the energy region $E_{c.m.}/V_B = 1$ to 1.5, where V_B is the Coulomb barrier height. There are no discrete ambiguities in values of the four optical parameters U, W, a, and r_0, and the continuous ambiguities are of the Igo type.[6] Also, as reported earlier,[4,5] fairly unique values are obtained for the Coulomb barrier height and radius, as discussed in the text. We have shown this uniqueness to be in the framework of an extended Igo ambiguity.

The standard Igo ambiguity, when used for the imaginary potential as well as the real potential, indicates that the ratio of real to imaginary potential well depths should be a constant for equivalent sets of optical model parameters within the ambiguity. We have demonstrated this effect over a two order of magnitude change in U. For a particular scattering system the uniqueness of any extracted value of the ratio, W/U, is in considerable question, however, as we have demonstrated its dependence on the quantity and quality of the data.

When a single folding procedure is used to generate the real part of the optical potential for different nickel isotopes, and when it is applied to data measured at different bombarding energies, no over-all improvement in the description of the data is achieved. Since this is true and in addition the number of parameters is nearly the same as in the conventional optical model description, the folding model description cannot at this point be considered as superior to the conventional one. The nucleon + projectile real potential depth within the target nucleus which is needed to describe ^{16}O + ^{58}Ni scattering data via a folding procedure is less than half the value needed to describe the free nucleon + ^{16}O scattering data. It is clear that additional theoretical work on the microscopic processes involved in heavy ion scattering is needed.

The authors wish to acknowledge Dr. J. L. Artz for his assistance during the data acquisition portion of this work and Dr. D. Robson and Dr. S. Cotanch for helpful discussions concerning the folding calculations.

---

*Work supported in part by the National Science Foundation Grants Nos. NSF-GP-25974 and NSF-GJ-367.

[1]J. A. McIntyre, S. D. Baker, and T. L. Watts, Phys. Rev. 116, 1212 (1959).

[2]J. Orloff and W. W. Daehnick, Phys. Rev. C 3, 430 (1971).

[3]B. C. Robertson, J. T. Sample, D. R. Goosman, K. Nagatani, and K. W. Jones, Phys. Rev. C 4, 2176 (1971).

[4]M. C. Bertin, S. L. Tabor, B. A. Watson, Y. Eisen, and G. Goldring, Nucl. Phys. A167, 216 (1971).

[5]A. W. Obst, D. L. McShan, and R. H. Davis, Phys. Rev. C 6, 1814 (1972).

[6]G. Igo, Phys. Rev. Lett. 1, 2 (1958); Phys. Rev. 115, 1665 (1959).

[7]P. Mailandt, J. S. Lilley, and G. W. Greenlees, Phys. Rev. C 8, 2189 (1973), and references therein.

[8]E. Heinicke, K. Bethge, and H. Baumann, Nucl. Instrum. Methods 58, 125 (1968).

[9]L. West, Jr., and N. R. Fletcher, unpublished.

[10]F. G. Perey, Phys. Rev. 131, 745 (1963); A. W. Obst, Florida State University Technical Report JIB, 1973 (unpublished).

[11]P. R. Bevington, *Data Reduction and Error Analysis for the Physical Sciences* (McGraw-Hill, New York, 1969).

[12]G. W. Greenlees, G. J. Pyle, and Y. C. Tang, Phys. Rev. 171, 1115 (1968).

[13]S. G. Kadmenski *et al.*, Yad. Fiz. 10, 730 (1969) [transl.: Sov. J. Nucl. Phys. 10, 442 (1970)].

[14]P. Schumacher, N. Ueta, H. H. Duhm, K. I. Kubo, and W. J. Klages, Nucl. Phys. A212, 573 (1973).

[15]S. Mackintosh, Nucl. Phys. A210, 245 (1973); S. Cotanch and L. West, Jr., unpublished.

[16]C. M. Perey and F. G. Perey, Nucl. Data A10, 539 (1973).

[17]R. Hofstader and H. R. Collard, in *Nuclear Radii Determined by Electron Scattering, Landolt-Bornstein,* edited by H. Schopper (Springer-Verlag, Berlin, 1967).

[18]D. C. Weisser, J. S. Lilley, R. K. Hobbie, and G. W. Greenlees, Phys. Rev. C 2, 544 (1970); P. P. Urone, L. W. Put, B. W. Ridley, and G. D. Jones, Nucl. Phys. A167, 483 (1971); M. E. Cage, D. L. Clough, A. J. Cole, J. B. A. England, G. J. Pyle, P. M. Rolph, L. H. Watson, and D. H. Worledge, ***ibid.*** A183, 449 (1972).